2014

Investigation On Premature Failure Of the Self-lubricated Piston Rings in Oil-free Compressor

Jinfeng Chen
Xi'an Jiaotong University, China, People's Republic of, chenjinfeng@stu.xjtu.edu.cn

Bin Zhao
Xi'an Jiaotong University, China, People's Republic of, zblqwy@163.com

Jianmei Feng
Xi'an Jiaotong University, China, People's Republic of, jmfeng@mail.xjtu.edu.cn

Xueyuan Peng
Xi'an Jiaotong University, China, People's Republic of, xypeng@mail.xjtu.edu.cn

Investigation on Premature Failure of the Self-lubricated Piston Rings in Oil-free Compressor

Jinfeng CHEN[1], Bin ZHAO[1], Jianmei FENG[1]*, Xueyuan PENG[1]
[1]School of Energy and Power Engineering, Xi'an Jiaotong University,
Xi'an ,Shaanxi, China
Corresponding author. Tel:+86 029 82665327
E-mail address: jmfeng@mail.xjtu.edu.cn

ABSTRACT

This paper presents the numerical simulation and experimental investigation on impact factors on premature failure of the self-lubricated piston rings in oil-free compressor. In this paper, the finite element method (FEM) was applied to study the non-uniform pressure distributions between the piston rings and the friction process between the self-lubricating piston rings and the cylinder wall, which influence the failure of the self-lubricated piston rings most. In order to verify the mathematic model, a test rig was built to measure the dynamic pressure distribution and temperature field between the piston rings. Both the theoretical and experimental results showed that the first piston ring afford more than 75% of the total pressure difference which was the main reason for the non-uniform wear and thus lead to early failure. The friction heat produced between the first piston ring and the cylinder was far more than the rest, which cannot be diffused rapidly through the low conductivity self-lubricating plastics and led to thermal failure of the self-lubricating piston rings. The results provide the theoretical basis to determine reasonably the design parameters and the thermal performance of piston rings.

1. INTRODUCTION

The oil-free compressors are widely applied in chemical, petrochemical, gas and general industry process, and the self-lubricating piston ring has a significant influence on the economy and reliability of the oil-free compressors. It is known that the piston rings are embedded into the piston to seal the high pressure differences. In theory, the pressure difference and wear on each ring are well proportioned to achieve the longest life for piston rings. However, in actual operations, certain rings appear to fail in advance due to their excessive loads and the resulting non-uniform pressure distribution1.

Several past studies have been conducted to investigate the friction and wear of piston rings in reciprocating machine. Some of them paid more attention to the dynamics of piston rings. Using the reciprocating tribometer, Johansson et al. investigated the impact of contact conditions on friction between the cylinder liner and piston ring, pointing out that the piston system accounted for approximately half of the mechanical friction in an internal combustion engine. Truhan et al. evaluated the friction and wear between the piston ring and cylinder liner of a heavy duty diesel engine under various conditions, including the use of different lubricants. Sutaria et al. performed numerical simulations on the piston ring friction in a single cylinder internal combustion engine and found that the friction rate was generally directly proportional to the piston speed. Furthermore, by studying the friction force between the piston ring and the cylinder bore in the bent-axis type of piston pump.Cho et al. concluded that the friction force was influenced by the rotating speed and the discharge pressure. On the other hand, some of the

studies focused on the material of self-lubricating piston rings, Unal et al. studied the influence of speed on the friction and wear behaviour of some industrial polymers against a steel counterface. Lewis tested a new PTFE-impregnated cloth material as a surface layer on the pistons of a hydraulic motor at the interface with the cam roller. Kowandy et al. investigated the wear particles, coefficients of friction and wear rates of three types of PTFE (pure and filled with glass fibre and carbographite) against flake grey cast iron to determine wearing mechanisms.

Although some of the above studies paid close attention to the piston rings dynamics and self-lubricated material by the experiment or simulation, none of them combine the numerical simulation and experimental to investigate the impact factors on premature failure of the self-lubricated piston rings in oil-free compressor. Considering the lack of this aspect of these studies, the finite element method (FEM) was applied to study the friction process between the self-lubricating piston rings and the cylinder wall, the frictional heat and the temperature distribution in the friction pairs were obtained from the simulated results. In order to verify the accuracy of simulation results, a special test rig was built by modifying an existing oil-free reciprocating compressor with a specially designed piston and cylinder in this paper.

2. MATHEMATIC MODEL

In this study, the compressor adopted in the simulation and experiment was a modified oil-free compressor, and its speed is 1500r·min-1; the material of piston is Aluminum Alloy, the material of piston ring is PTFE, and the material of cylinder、cylinder head、valve plate etc is ductile iron.

2.1 Temperature Field

In order to effectively simulate the temperature field in the oil-free compressor, we should analysis the heat exchanges of the oil-free compressor firstly. As is known that the heat exchanges in the oil-free compressor occurs in four ways. Forced convection heat transfer occurs between the gas in the compressor, suction or exhaust chambers and the inner surface of the cylinder; natural convection heat transfer takes place between the ambience and the outer surface of the cylinder; natural convection heat transfer takes place between the ambience and the outer surface of the cylinder; frictional heat generation and conduction happens between the piston rings and the inner surface of cylinder; thermal conduction happens between the middle body and the cylinder.

Based on the above analysis, two assumptions were made to effectively simulate the temperature field: (1) Properties of the cylinder materials were homogeneous and did not change with different temperatures; (2) The friction coefficient between the piston rings and the cylinder was constant and all of the frictional work was converted into heat.

As the cylinder was a perfectly symmetrical structure, only a semi-cylinder was analyzed to better observe the temperature field, and the FEM model of the cylinder, piston and piston ring were shown in Fig. 1.

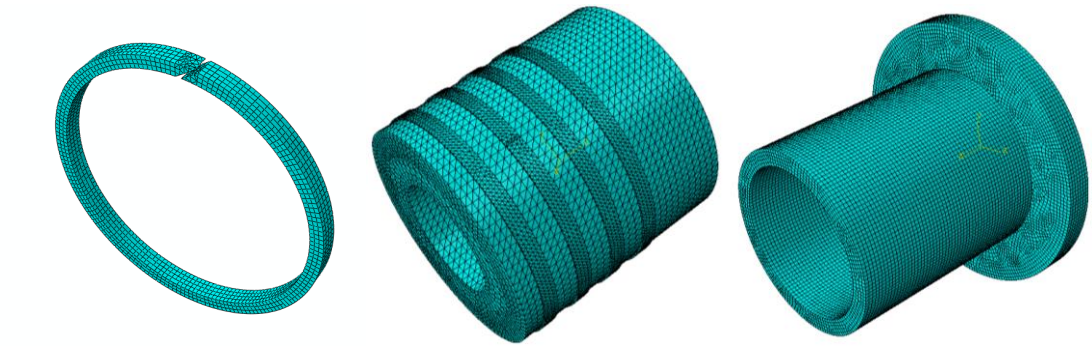

Figure 1: The FEM model

2.2 Non-uniform Pressure Distributions

In this paper, the severe non-uniformity of pressure distribution had been suggested as the essential reason for the premature failure of the piston rings in oil-free compressors. The flow through the cuts of piston rings was presumed as one-dimensional compressible isentropic flow through a convergent-divergent nozzle, and the mathematical model was established to simulate the unsteady flow within the gaps of piston rings by the control volume method on the basis of energy conservation equation and mass conservation equation.

The volume formed by the piston before the piston ring and the inner surface of cylinder is much larger than the leakage from the ring cut. For this reason, the whole flow of the piston ring group can be simplified as one-dimensional compressible adiabatic flow of multiple series expansion chamber. The simplified model is shown in Fig. 2.

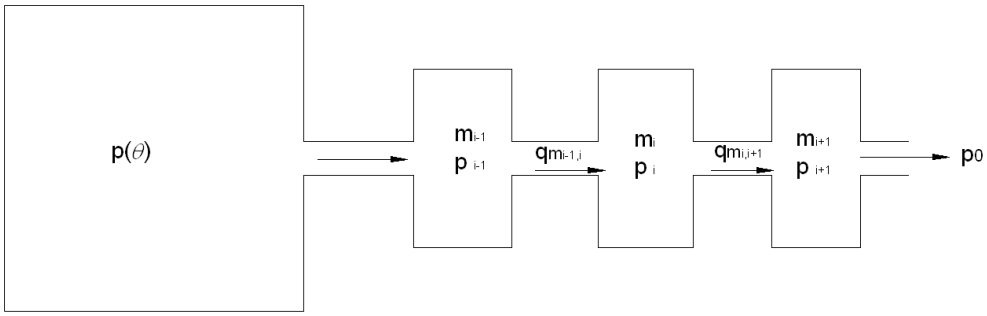

Figure 2: The Mathematic model of pressure distributions between the piston rings

3. EXPERIMENT

3.1 Experimental Set-up

To obtain the friction process and the actual pressure distributions between the piston rings, a test rig was built by modifying the existed oil-free reciprocating compressor with a specially designed piston and cylinder. Self-lubricating piston rings were used. The schematic diagram of this test rig is shown in Fig. 3 (a). The specially designed piston and cylinder are shown in Fig. 3 (b). The compression chamber was on the crankshaft side so that the signal wires could be led out from the cylinder cover side. The piston comprised several annular piston pieces with a ladder-like external surface. Two neighboring piston pieces formed a piston ring groove and an O-ring was used to seal between them. As the integrated piston was hollow, the dynamic pressure sensors between the piston

rings could be embedded into the piston and the wires of the sensors could be led out, as shown in Fig.4. The pressure sensors were arranged to record the dynamic pressures in the volumes between the piston rings for further processing in the data acquisition system. The pressure sensors, together with the signal wires, were all fixed to the piston, so that they moved with the piston during the operation of the compressor.

The pressure sensor's uncertainty was less than $\pm$0.1% and its response frequency was as high as 550 kHz. The maximum working pressure was 1.7MPa, and the dynamic data acquisition system was based on an acquisition card with a sampling frequency of 1MHz. The analogue input of the acquisition card was up to 16 simultaneous ways and the maximum sampling frequency of a single channel 250 kHz.

The piston rings were made of filled PTFE and the material of the cylinder was nodular cast iron. The sealing set included four piston rings and one rider ring. The piston rings were named first, second, third and fourth in sequence from the high-pressure to the low-pressure side, with the pressures before them defined as p0, p1, p2 and p3, respectively. The pressure between the fourth ring and the rider ring was defined as p4.

The pressure distributions were measured as the compressor was operating at atmospheric pressure and 0.3MPa of the suction pressure while the pressure ratio was kept at about 3.0. Based on the test results, the contact position of the piston rings and the formation process of the pressure difference on the rings were discussed.

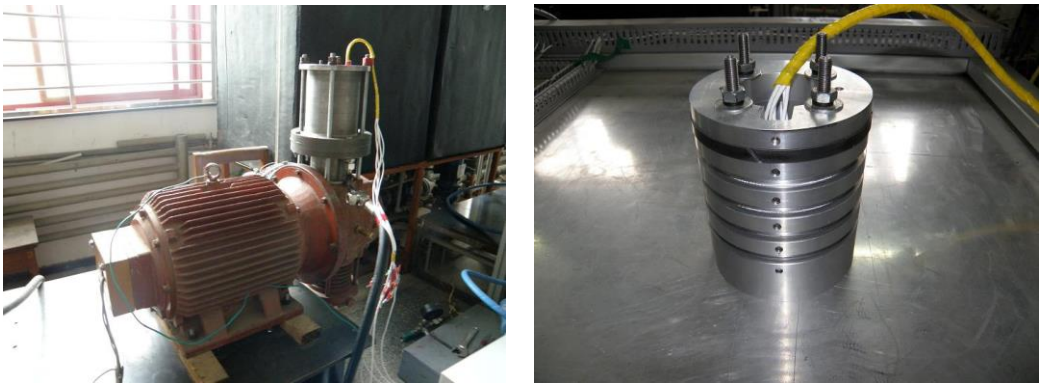

a) The schematic diagram b) Piston and dynamic pressure sensors

Figure 3: The test rig

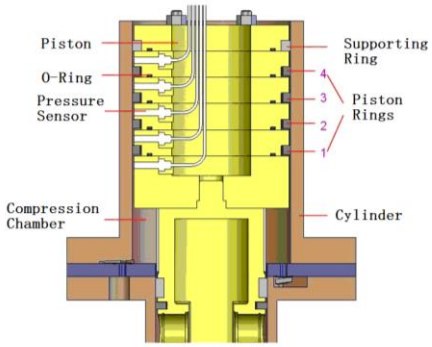

Figure 4: Cut view of the test device

3.2 Uncertainty Analysis

According to the uncertainty theory [13], the combined standard uncertainty in measurement is the positive square root of the variance.

$$u_c^2(y) = \sum_{i=1}^{N} (\frac{\partial f}{\partial x_i})^2 u^2(x_i)$$

where $u(x_i)$ represents the uncertainty of the calculated quantity and x_i the individual measurements.

For this experiment, the combined uncertainty was mainly associated with the uncertainty of the pressure sensor and the data acquisition system, which were, respectively, 0.1% and 0.03%, so that the combined uncertainty was about 0.11%.

4. RESULTS AND DISCUSSION

4.1 Friction Process

The finite element method (FEM) was applied to study the friction process between the self-lubricating piston rings and the cylinder wall, and the frictional heat and the temperature distribution in the friction pair were obtained from the simulated results. The influence of its thermal conductivity on the temperature field of the self-lubricating piston ring was analyzed and the distribution of the frictional heat between the self-lubricating piston rings and the cylinder was discussed. The simulated temperature field of the cylinder, piston and piston rings were shown in Fig. 5, from which it can be observed that the highest temperature of friction pairs was 376K, and the frictional heat distributed to the piston rings occupied a small fraction.

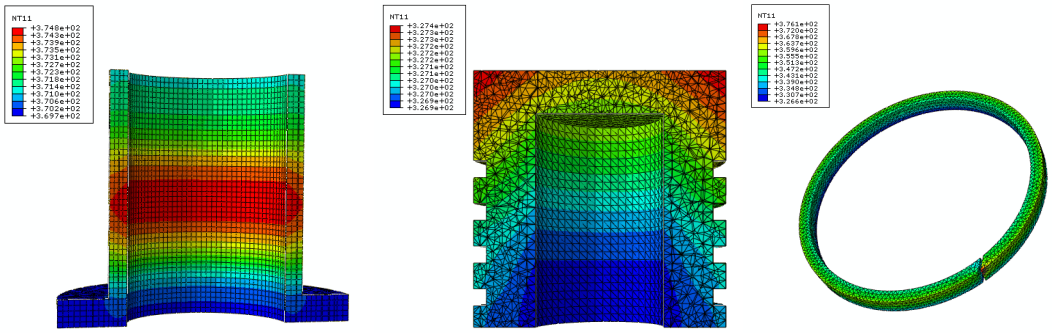

a) Cylinder b) Piston c) The first piston ring

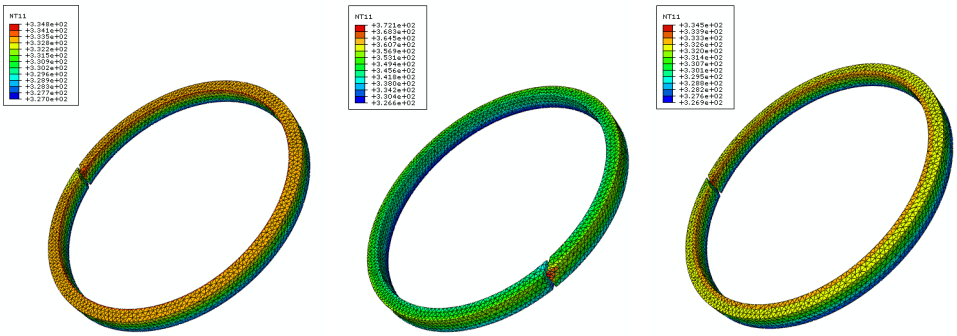

d) The second piston ring e) The third piston ring f) The fourth piston ring

Figure 5: Simulated temperature of the cylinder, piston and piston rings

By varying the thermal conductivity coefficient of piston rings, the temperature fields were studied so as to identify the main factors that influenced the friction process most. In order to study the influence of temperature field in piston rings from material thermal conductivity coefficient, this paper adopted three different material piston rings. The physical parameters is shown in Table 1, and the simulate temperature field of piston rings in Table 2.

Table 1: Physical parameters of different material

conditions	PTFE	Victrex-450GL30	Victrex-450CA30
Friction coefficient	0.1	0.16	0.26
density/kg m-3	2200	1510	1410
Specific heat/J (kg K)-1	1000	1700	1800
thermal conductivity coefficient /W (m K)-1	0.25	0.43	0.92

Table 2: The simulated temperature field of piston rings

conditions	PTFE	Victrex-450GL30	Victrex-450CA30
distribution of the frictional heat	0.065	0.1	0.24
The highest temperature of friction pair /K	376	411	466
Inner/outer surface temperature of first piston ring/K	346/363	356/372	360/372
Inner/outer surface temperature of second piston ring /K	334/333	335/335	307/307
Inner/outer surface temperature of third piston ring /K	345/355	354/370	349/377
Inner/outer surface temperature of fourth piston ring /K	333/332	334/333	305/304

The flowing conclusions can be obtained by comparing physical parameters with simulate results. The frictional

heat distributed to the piston rings increased with the increasing of the thermal conductivity coefficient of the self-lubricating materials. The highest temperature of friction pair increased with the increasing of the material friction coefficient.

4.2 Pressure Distribution

It is known that the sealing effect of a piston ring depends on the pressure difference acting on it; without such a pressure difference it will not work. It is necessary to examine the formation of the pressure difference to figure out the root cause of the non-uniformity of the pressure distributions that has such an adverse effect on the piston rings' lifetime.

4.2.1 Static operation conditions

Fig. 6 shows the generation of pressure difference between the piston rings when the compression chamber was filled and discharged. As shown in Fig. 6, the pressure before each ring did not increase simultaneously when the compression chamber was filled with air. In this process, the pressure before the first ring (p0) increased continually, while the pressures before other rings (p1 and p2) did not, at first, increase in the same way. When the pressure before the first ring reached a certain value (~2.5 bar), the pressure before the second ring (p1) began to increase, indicating that the second ring started working at this point. Similarly, the pressure before the third ring (p2) did not change until that before the second ring reached a certain value (~3.7 bar), showing the third ring's onset working time. This provided conclusive evidence that in terms of sealing, each piston ring did not work simultaneously and could not function until the pressure before it achieved the particular value necessary to form the required pressure difference. Furthermore, it is also clear that when the gas was discharged from the compression chamber, the piston rings did not simultaneously become failed. At first, the pressures in all the volumes between the rings decreased, but when the pressure in the cylinder was very low, the third ring failed first, followed by the second and the first.

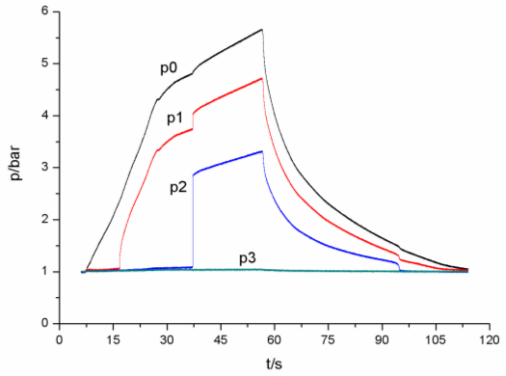

Figure 6: Pressure distribution as the static pressure difference formed.

Fig. 7 shows the schematic diagram for the working of the piston rings, explaining why they cannot work simultaneously. When the piston ring works normally, its outer face comes into close contact with the cylinder's internal surface by the action of the gas force and the piston ring's end face is in complete contact with piston ring groove face, as shown by ring 1 in Fig. 7. At this time, the only gas leakage path is that of the ring cut, and so the piston ring is able to seal the gas effectively.

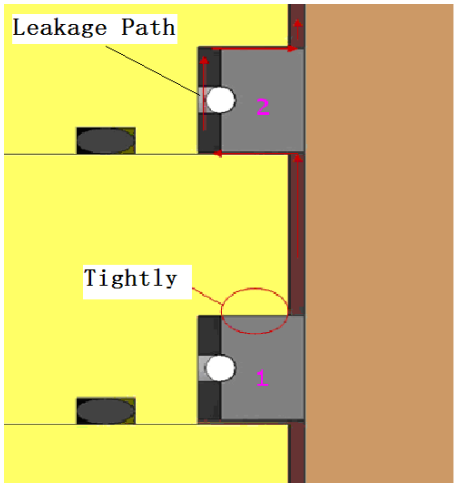

Figure 7: Schematic diagram for the working of the piston rings

4.2.2 Dynamic operation condition.

The pressure distribution between the piston rings indicated that the alternative contact positions of the piston rings exerted an insignificant influence on the pressure distribution. However, the repeated impacts led to the premature ring failure due to material fatigue.

To investigate the working conditions of the rings at the high-pressure stage, in which the suction pressure usually exceeds the pressure in the crank case, the experiment was conducted at the suction pressure of 0.3MPa and the pressure ratio ~3.0. The recorded pressure distribution at the high-pressure stage was different from that at the low-pressure one, as shown in Fig. 8. When the total pressure difference was increased to 1.3MPa, the first ring still bore most of the pressure difference (about 75%), but the other rings did not work until the pressure difference reached a specific level. The experimental data showed that the second and last rings both took approximately 10% of the total pressure difference, and the third ring bore the least pressure difference (about 5%). That pressure distribution was used to derive the axial reaction force, Fp, with the results presented in Fig.9

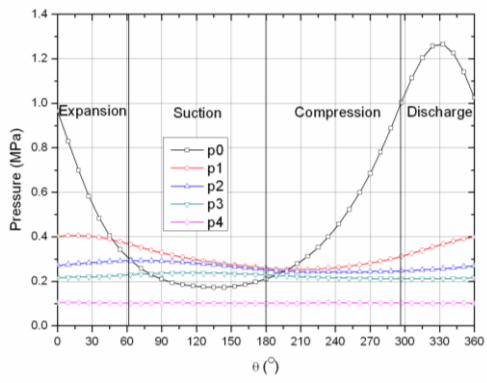

Figure 8: Pressure distribution at high-pressure stage (ps=0.3MPa, pd=1.0MPa)

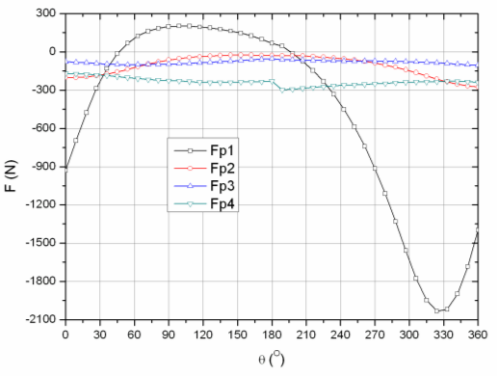

Figure 9: Axial reaction forces on piston rings at high-pressure stage.

At the low-pressure stage, the pressure difference on the first piston ring could be established immediately as the compressor was starting up, but there was hardly any formation of pressure difference on the other rings. However, at the high-pressure stage, the pressure difference on each ring could be established at different degrees, as shown in Fig. 9, nothing else than establishment at the same time. This shows that all the rings cannot work simultaneously. Figure8 shows the pressure distribution as the dynamic pressure difference forms; Fig. 10 (b) and (c) are the partially enlarged graphs of Fig. 10 (a). At first, the pressure difference only appeared on the first and second rings. As the pressure in the working chamber increased, the fourth ring began to function and bear the pressure difference, as shown in Fig. 10 (a) and (b). As the pres- sure continued to increase, the pressure difference also formed on the third ring, as can be seen in Fig. 10 (a) and (c). The results confirmed that the ring began to seal the gas leakage only when the pressure difference on it had reached a certain value. The special test, described in the following section, was performed in the same compressor for further verification.

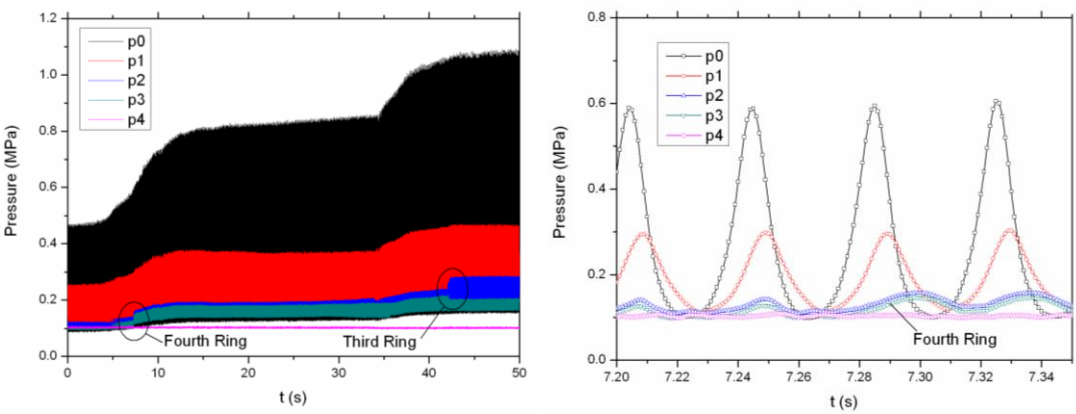

(a) (b)

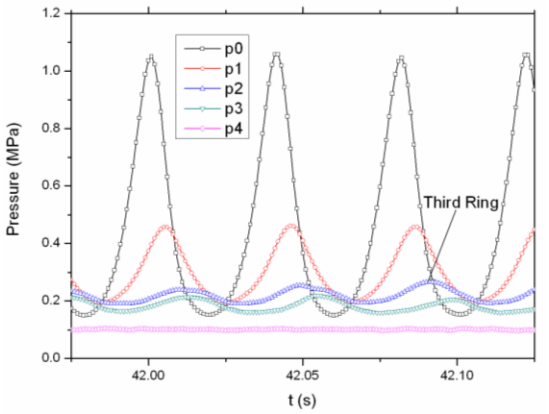

(c)

Figure 10: Pressure distribution as the dynamic pressure difference formed

5. CONCLUSIONS

The finite element method was used to obtain the non-uniform pressure distributions between the piston rings and the friction process between the self-lubricating piston rings and the cylinder wall, and the results agreed with the experimental results. Therefore, the FEM can be used to effectively simulate pressure distributions and friction process of piston rings in oil-free compressors.

1. The frictional heat distributed to the piston rings increased with the increasing of the thermal conductivity coefficient of the self-lubricating materials. The thermal conductivity coefficient of the filling component was observed to be proportional to the quantity and thermal conductivity of the filling particles, but had no direct relationship with the filler's size.

2. In the high-pressure stage of the compressor, where the suction pressure exceeded the pressure in the crank case, most of the pressure difference (about 75%) was on the first piston ring; the second and last rings also took about 10% of the total pressure difference, and the third ring bore the least pressure difference (about 5%). This phenomenon was not the same as that in the first stage, where the suction pressure was close to the pressure in the crank case.

3. The seal mechanism of the piston ring prevented the pressure differences between the rings from forming at the same time. This implied that each piston ring began to work only when the pressure difference on it reached a required value, which contributed to the non-uniform pressure distributions and short life-time of the whole piston ring set.

REFERENCES

Tian, T., 2002, Dynamic behaviors of piston rings and their practical impact part 1: ring flutter and ring collapse and their effects on gas flow and oil transport, *Proc IMechE Part J J Engineering Tribology*, vol. 216, no. 4: p. 209–228.

Cho JR., Moon SJ., 2005, A numerical analysis of the interaction between the piston oil film and the component deformation in a reciprocating compressor, *Tribol Int*, vol. 38, no. 5: p. 459–468.

Meng FM., Wang JX and Xiao K., 2010, A study of the influences of particles in the gas flow passage of a piston ring pack on the tribological performances of the piston ring, Proc IMechE Part C J Mechanical Engineering Science, vol. 224, no 1: p. 201–215.

Yang B. and Zhao Y., 2011, Piston ring–cylinder liner lubrication analysis in a CO2 refrigeration reciprocating compressor, Proc IMechE Part C J Mechanical Engineering Scienc., vol. 225, no 11: p. 2638–2648.

Johansson S, Nilsson PH, Ohlsson R, et al. 2011, Experimental friction evaluation of cylinder liner/piston ring contact. Wear 2011, vol. 271, no. 3–4: p. 625–633.

Johansson S, Frennfelt C, Killinger A, et al. 2011, Frictional evaluation of thermally sprayed coatings applied on the cylinder liner of a heavy duty diesel engine: pilot tribometer analysis and full scale engine test. Wear 2011, vol. 273,no. 1: p 82–92.

Truhan JJ, Qu J and Blau PJ, 2005, A rig test to measure friction and wear of heavy duty diesel engine piston rings and cylinder liners using realistic lubricants. Tribol Int 2005, vol. 38, no. 3: p. 211–218.

Sutaria BM, Bhatt DV and Mistry KN, 2009, Simulation of piston ring friction models of a single cylinder internal combustion engine. World Appl Sci J, vol. 7, no. 8: p. 998–1003.

Cho I, Beak I, Jo J, et al. 2010, Lubrication characteristics of dual piston ring in bent-axis type piston pumps. J Mech Sci Technol, vol. 24, no. 6: p. 1363–1368.

Unal H, Sen U and Mimaroglu A, 2004, Dry sliding wear characteristics of some industrial polymers against steel counterface. Tribol Int, vol. 37, no. 9: p. 727–732.

Lewis R, 2009, Friction in a hydraulic motor piston/cam roller contact lined with PTFE impregnated cloth. Wear, vol. 266, no. 7–8: p. 888–892.

Kowandy C, Richard C and Chen YM, 2008, Characterization of wear particles for comprehension of wear mechanisms case of PTFE against cast iron. Wear, vol. 265, no. 11–12: p. 1714–1719.

International Organization for Standardization (ISO), 1995, Guide to the expression of uncertainty in measurement. Geneva: International Bureau of Weights and Measures, ISO.

ACKNOWLEDGEMENTS

This study was supported by the National Natural Science Foundation of China (Research Project 51175407/E050501).